Open Journal of Inorganic Chemistry, 2012, 2, 6-11 **OJIC**
http://dx.doi.org/10.4236/ojic.2012.21002 Published Online January 2012 (http://www.SciRP.org/journal/ojic/)

Preparation mechanism and luminescence of Sr_2SiO_4:Eu phosphor from (Sr,Eu)CO_3@SiO_2 core-shell precursor

Yunsheng Hu[1], Weidong Zhuang[1*], Jianhua Hao[2*], Xiaowei Huang[1], Huaqiang He[1]

[1]National Engineering Research Center for Rare Earth Materials, General Research Institute for Nonferrous Metals, and Grirem Advcanced Materials Co., Ltd., Beijing, China
[2]Department of Applied Physics, The Hong Kong Polytechnic University, Hong Kong, China
Email: [*]wdzhuang@126.com; [*]apjhhao@polyu.edu.hk

Received 2 November 2011; revised 8 December 2011; accepted 21 December 2011

ABSTRACT

Sr_2SiO_4:Eu phosphor for white light emitting diodes (LEDs) was synthesized by employing an as-prepared (Sr,Eu)CO_3@SiO_2 core-shell precursor as starting materials, and the effect of the core-shell precursor was also discussed on the crystal structure, particle morphology and luminescent properties of the resultant phosphor. The results showed that the hybrid β- and α'-Sr_2SiO_4: Eu phosphor with fine particle size and narrow distribution could be obtained at a lower firing temperature than that in conventional solid-state reaction method, and its formation mechanism was deduced to be (Sr,Eu)CO_3 diffusion controlled reaction process. Responded to its hybrid crystal structure, this phosphor exhibited the combined luminescence of β- and α'-Sr_2SiO_4:Eu.

Keywords: Phosphor; Precursor; Core-Shell Structure; Preparation Mechanism; Luminescence

1. INTRODUCTION

Since Eu^{2+}-activated alkaline earth orthsilicate phosphor was firstly reported on its fluorescence by Barry in 1968 [1], Me_2SiO_4:Eu (Me = Ca, Sr, Ba) had attracted little attention until the advent of white light emitting diodes (LEDs). Due to its high light conversion efficiency for near ultraviolet (NUV) and blue light, Me_2SiO_4:Eu has been an excellent commercial phosphor for white LEDs. Compared with the most popular $(Y,Gd)_3(Al,Ga)_5O_{12}$:Ce (YAG:Ce) phosphor for white LEDs, Me_2SiO_4:Eu is not only suitable for blue LED but also for NUV LED; moreover, Me_2SiO_4:Eu can produce more colorful emission to satisfy the demands of the white LEDs with lower color temperature and higher color rendering index [2-6].

Currently, the commercial Me_2SiO_4:Eu phosphor is produced by high temperature solid-state reaction method [5-10]. Such a method can achieve high light conversion efficiency of phosphor; however, it usually requires high firing temperature and introduction of flux to promote crystallization, which results in big particle size (>10 μm), broad particle distribution and irregular morphology, even flux contamination for phosphor. Taking the application properties into account, the phosphors for LEDs should have suitable particle size (<10 μm) and narrow distribution besides high brightness and desirable color coordinates. So some efforts have made to improve the particle properties of Me_2SiO_4:Eu phosphor by soft-chemistry methods [11-14]. For instance, Chang and co-authors synthesized nanometer Sr_2SiO_4 by employing $SrCO_3$@SiO_2 core-shell precursor as the starting materials; however, the luminescent center Eu was not considered and doped into the Sr_2SiO_4 host in their work [14]. In the previous work, we also developed a homogenous (Sr,Eu)CO_3@SiO_2 core-shell precursor, in which (Sr,Eu)CO_3 represents the homogenous mixture of Sr^{2+} and Eu^{3+} carbonates [15]. In this study, we employed this as-prepared core-shell precursor as starting materials to synthesize Sr_2SiO_4:Eu phosphor, and investigated its effect on the crystal structure, morphology and luminescent properties of the phosphor. Based on these results, the formation mechanism and the luminescence of Sr_2SiO_4:Eu was also discussed.

2. EXPERIMENTAL

The as-prepared (Sr,Eu)CO_3@SiO_2 core-shell precursor in our previous work [15] was directly employed as the starting materials to synthesize Sr_2SiO_4:Eu phosphor in the present work, wherein the molar ratio of Sr, Eu and Si was 1.9:0.1:1. To be specific, the core-shell precursor was put into an alumina crucible and directly fired in a horizontal tube furnace at 1000˚C for 2 h under reducing atmosphere (95% N_2 + 5% H_2). And then the obtained phosphor powder was cooled to room temperature in the furnace for characterization.

FTIR measurements were performed on a Nicolet Magna-IR 760 Fourier transform infrared spectrometer

[*]Corresponding authors.

using the standard KBr pellets technique, in the frequency interval 4000 - 400 cm^{-1}. X-ray diffraction (XRD) identification was determined by Burker D8 Advance X-ray powder diffractometer running Cu Kα radiation at 40 kV and 40 mA, and the XRD patterns were collected in the range of $15^{\circ} \leq 2\theta \leq 65^{\circ}$. The microstructure and morphology were detected by a JEOL JSM-6335F field emission scanning electronic microscope. The emission and excitation spectra of the phosphor were acquired by using Edinburgh FLS920P fluorescence spectrometer equipped with a 450W xenon lamp as an excitation source. All the measures were carried out at room temperature.

3. RESULTS AND DISCUSSION

Figure 1 shows the FTIR spectrum of the obtained phosphor sample (curve b). For comparison, the FTIR spectrum of (Sr,Eu)CO_3@SiO_2 precursor is also presented as curve (a). Obviously, the FTIR spectrum of the precursor mainly exhibits the characteristic vibrations of SiO_2 (1093, 796 and 471 cm^{-1}), CO_3^{2-} group (692, 856, 1456 and 1749 cm^{-1}), CTAB (1630 and 2823 cm^{-1}) and H_2O (3435 cm^{-1}). After the precursor was fired into phosphor, the obtained sample shows different FTIR spectrum. As displayed in curve (b), the characteristic vibrations of CO_3^{2-} group, CTAB and H_2O disappear, and the characteristic vibration bands of SiO_2 are replaced by multiple bands at 1000 - 800 cm^{-1} and 600 - 500 cm^{-1}, which could be attributed to the stretching and bending vibrations of Si-O bonds in SiO_4 tetrahedra, respectively [16]. It means that the vibration bands of the phosphor sample are shifted to lower frequency compared with that of pure SiO_2. As O/Si ratio increases from 2 (SiO_2) to 4 (orthosilicate), the Si-O bond length increases from 0.161 nm to 0.163 nm due to the presence of modifier oxides in the silica network, and the polymerization degree of SiO_4 tetrahedral gets lower, which generally corresponds to a lower vibration frequency in FTIR spectrum [17,18]. Meanwhile, it is noticed that the stretching vibrations of the phosphor sample cover a broader range (1300 - 600 cm^{-1}, the region between both dot lines in curve (b)) than that of pure SiO_2 (1300 - 880 cm^{-1}, the region between both dot lines in curve (a)) and split into three groups: 962, 908, and 839 cm^{-1}, which is probably arisen by the di- fferent NBO/Si ratio (NBO/Si: non-bridging oxygen per silicon) in SiO_4 tetrahedra [19].

To further investigate and clearly identify the phase structure, **Figure 2** depicts the XRD pattern of the phosphor sample obtained by directly firing (Sr,Eu)CO_3@SiO_2 precursor at 1000˚C for 2 h. This pattern agrees well with the standard diffraction data of α'-Sr_2SiO_4 (JCPDS No. 39-1256) and β-Sr_2SiO_4 (JCPDS No. 38-0271), so it can be deduced that this phosphor sample is a mixture of

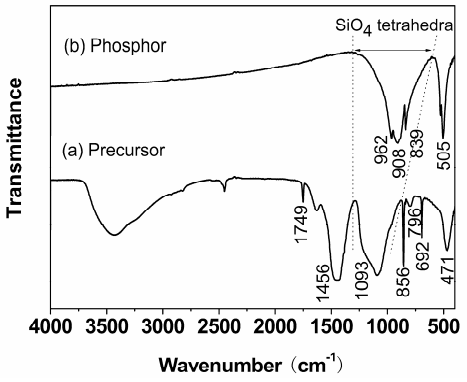

Figure 1. FTIR spectra of (Sr,Eu)CO_3@SiO_2 precursor (a) and the obtained Sr_2SiO_4:Eu phosphor sample (b).

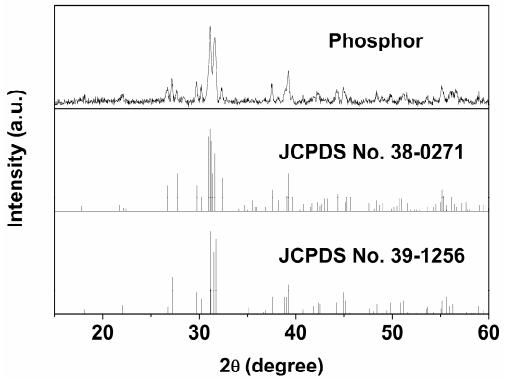

Figure 2. XRD pattern of Sr_2SiO_4:Eu phosphor sample prepared by directly firing (Sr,Eu)CO_3@SiO_2 precursor at 1000˚C for 2 h.

orthorhombic α'-Sr_2SiO_4:Eu and monoclinic β-Sr_2SiO_4:Eu. The α' and β forms are the two modifications of Sr_2SiO_4, and the phase transition between low temperature β phase and high temperature α' phase occurs at about 358 K [20,21], whereas α' phase can also be stabilized at room temperature by substituting more Eu ($\geq$0.1) or small amounts of Ba^{2+} for Sr^{2+} [22,23]. In this work, the concentration of Eu activator is 0.1, so α'-Sr_2SiO_4:Eu is stably crystallized as well as β-Sr_2SiO_4:Eu as expected. Approximately estimated from the intensity of the diffraction peaks, α'-Sr_2SiO_4:Eu has much more content percentage than β-Sr_2SiO_4:Eu in this mixture. It is noted that not only is the present synthesized temperature (1000˚C, no flux) lower than that in the conventional flux-assisted solid-state reaction method (usually 1300˚C), but also the contamination of flux can be avoided due to the absence of flux.

To investigate the effect of core-shell precursor on the morphology of the resultant Sr_2SiO_4:Eu phosphor, **Figure 3** and **Figure 4** demonstrate the SEM images of the precursor and phosphor sample, respectively. In this precursor (**Figure 3**), most of SiO_2 are induced to coat on

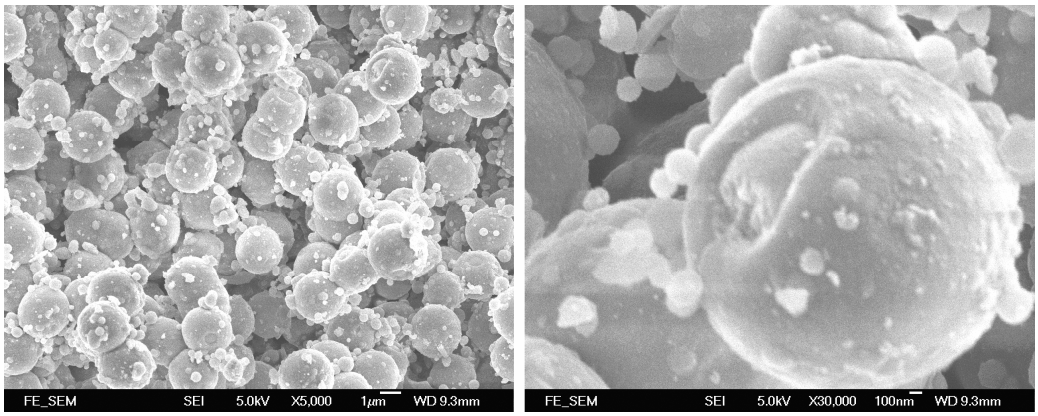

(a) (b)

Figure 3. SEM images of (Sr,Eu)CO_3@SiO_2 core-shell precursor observed at different magnifications: (a) × 5000; (b) × 30,000.

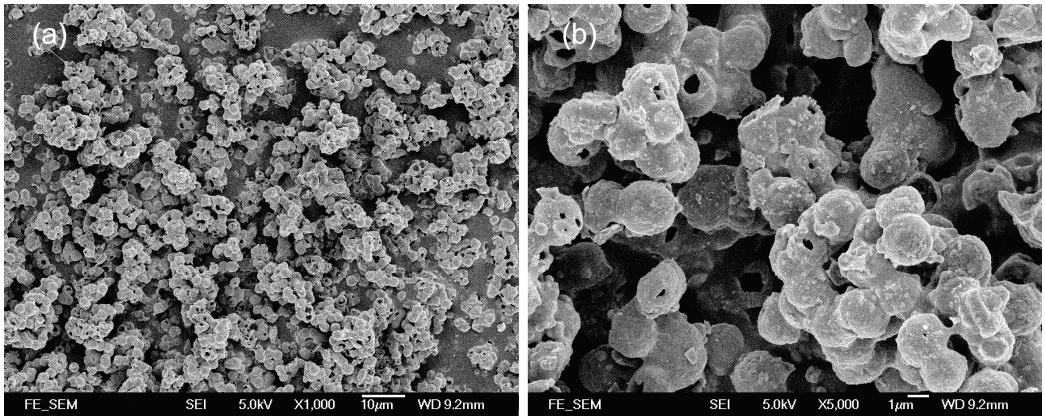

Figure 4. SEM images of Sr_2SiO_4:Eu phosphor sample observed at different magnifications: (a) ×1000; (b) × 5000.

the surface of (Sr,Eu)CO_3 core to form (Sr,Eu)CO_3@SiO_2 core-shell structure with SiO_2 shell layer about 100 ~ 200 nm thickness; however, a few nucleate directly into SiO_2 nano-particles (100 ~ 200 nm) and locate onto the surface of core-shell structure. The formation mechanism and the composition of this precursor have been disclosed in our previous work [15]. It can be noted that this precursor has imperfect core-shell structure, and there appears an apparent gap without coated by SiO_2 on every core-shell particle. However, the existence of the gap accesses us to clearly understand the reaction mechanism between core and shell by morphology observation and comparison.

After the precursor was fired at 1000˚C for 2 h, the obtained Sr_2SiO_4:Eu phosphor sample seems to inherit the external contour of the precursor. Overall, the particles of the phosphor still appear uniform and near-spherical morphology, as shown in **Figure 4(a)**, and the particle size is about 2 μm, slightly less than that of the precursor, which results from the condensation reaction between (Sr,Eu)CO_3 core and amorphous SiO_2 shell at the high temperature. Observed from the enlargement figure (**Figure 4(b)**), the condensation reaction also leads to slight aggregation and adhesion among particles, but the profile of the single particle can be clearly recognized, which indicates that every (Sr,Eu)CO_3@SiO_2 particle in the core-shell precursor would act as a separate reaction unit, and it is of the suitable stoichiometrical ratio to situ produce an isolated Sr_2SiO_4:Eu micrometer particle. More noticeably, all the particles of the Sr_2SiO_4:Eu phosphor exhibit hollow morphology with an opening, and the wall thickness is slightly thicker than that of SiO_2 shell layer of the precursor. Combined with the results of XRD analysis, it seems that the shell of the precursor has transformed into thicker Sr_2SiO_4:Eu layer, while the core has disappeared past the chemical reaction at the high temperature. That is to say, the fact that the phosphor particles still maintain near single and hollow spherical shape suggests that (Sr,Eu)CO_3 would diffuse into SiO_2 shell and react into hollow Sr_2SiO_4:Eu phosphor until the exhaust of (Sr,Eu)CO_3 core. It can be deduced intuitively that this reaction mechanism can be regarded as (Sr,Eu)CO_3

diffusion controlled process, which is consistent with the theoretical inference in Lu and Wu' work [24].

The luminescent properties of α'-Sr_2SiO_4:Eu or β-Sr_2SiO_4:Eu have been researched widely [25-28]; however, the hybrid luminescence of the co-existent phase of α'- and β-Sr_2SiO_4:Eu has seldom been separately distinguished. In order to systematically understand the dependence of luminescent properties on the crystal structure of Sr_2SiO_4:Eu phosphor, we further investigated and analyzed the photoluminescence of this hybrid phosphor sample.

Figures 5(a) and **(b)** show the emission and excitation spectra of the phosphor sample, respectively. As illustrated in **Figure 5(a)**, the peak of the dominant emission band moves from 555 to 568 nm with the increase of the excitation wavelength from 320 to 450 nm. Whichever the excitation wavelength is, a turn at 532 nm is observed in the emission spectra as clearly shown in the inset of **Figure 5(a)**, which implies that the peak at 532 should be classified as a different emission band from the dominant one in the emission spectra. Both emission bands are the response to the co-existence of α'-Sr_2SiO_4:Eu and β-Sr_2SiO_4:Eu. The orientations of β and α' lattices are related by a simple rotation of x axis, and β-Sr_2SiO_4:Eu with stronger Si-O bond valence produces stronger crystal field and then yields shorter wavelength emission compared with α'-Sr_2SiO_4:Eu, so it can be deduced that the emission band centered at 532 nm originates from β-Sr_2SiO_4:Eu, and its emission peak position is independent on the excitation wavelength; while the dominant emission band at longer wavelength should be ascribed to α'-Sr_2SiO_4:Eu, and this emission can occur blue- or red-shift with the change of the excitation wavelength. It can be noted that α'-Sr_2SiO_4:Eu shows stronger emission intensity than β-Sr_2SiO_4:Eu in our sample, which is contrary to the results confirmed by many work [10,22,26]. The reason is that α'-Sr_2SiO_4:Eu has much more mass percentage than β-Sr_2SiO_4:Eu in this phosphor sample. Both of the emission band are produced by the 5d-4f transition of the activator Eu^{2+} occupied the ten oxygen coordinated Sr^{2+}(I). As well known, there is another Sr^{2+} site, Sr^{2+}(II), surrounded by nine oxygen in β- and α'-Sr_2SiO_4:Eu. When Eu^{2+} replaces Sr^{2+}(II), a shorter blue light emission band will be produced with peak at about 470 nm. As shown in **Figure 5(a)**, the 470 nm blue emission is obviously resolved as gibbous shoulder when the excitation wavelength is as short as 320 nm, while it disappears when the excitation wavelength is set at 400 or 450 nm. On the other hand, the phosphor sample has the strongest emission peak intensity when excited by 400 nm (NUV, near ultraviolet), and the intensity still maintains about 80% under 450nm blue light excitation. That is to say, the Sr_2SiO_4:Eu phosphor can applied to combine with NUV-LED or blue LED.

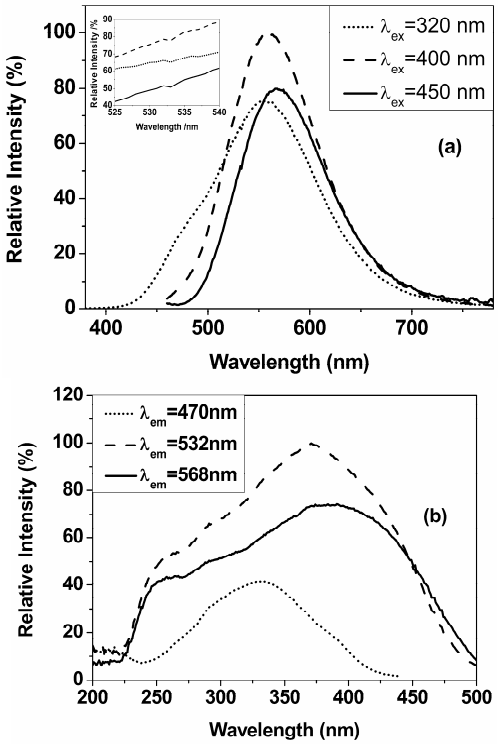

Figure 5. Emission (a) and excitation (b) spectra of the obtained Sr_2SiO_4:Eu phosphor sample.

The applicability of this Sr_2SiO_4:Eu phosphor for white LED can also be certificated by the excitation spectrum. Three excitation spectra were illustrated in **Figure 5(b)**, with monitoring emission wavelength at 568, 532 and 470 nm, respectively. Obviously, there is a very broad excitation band in 300 - 500 nm spectral regions when monitoring wavelength at 532 and 568 nm, which assures that this phosphor has high efficient light conversion for NUV and blue light. As for 470 nm blue emission, it has much lower efficiency, and its suitable excitation region is narrower (250 - 400 nm). That is the reason that 470 nm emission is nearly unresolved when this phosphor is excited by long-wavelength light.

4. CONCLUSIONS

The hybrid α'- and β-Sr_2SiO_4:Eu phosphor was successfully developed by firing (Sr,Eu)CO_3@SiO_2 core-shell precursor directly at 1000˚C, and it appeared uniformly hollow near-spherical morphology with particle size about 2 μm. The morphology was resulted from the core-shell structure of the precursor and the reaction mechanism between (Sr,Eu)CO_3 core and SiO_2 shell. The mechanism was acquired visually to be (Sr,Eu)CO_3 diffusion controlled reaction process. Responded to its hybrid crystal structure, the phosphor exhibited the combined luminescence of α'- and β-Sr_2SiO_4:Eu. α'-Sr_2SiO_4:Eu

has the longer emission wavelength, and its emission peak can blue- or red-shift with the change of the excitation wavelength; while the 532 nm emission of β-Sr_2SiO_4:Eu is independent on the excitation wavelength. Compared with the conventional high temperature solid-state reaction method, this method requires lower firing temperature and no flux contamination, and produces finer particles with narrow size distribution. More importantly, the reaction mechanism will provide some ideas to improve the particle performance of silicate phosphors, for instance, the spherical and solid Sr_2SiO_4:Eu phosphor could be obtained by employing a spherical SiO_2@ (Sr,Eu)CO_3 core-shell precursor as starting materials.

5. ACKNOWLEDGEMENTS

The authors would like to acknowledge the support from the National Hi-Tech. R&D Program of China (863 Program, 2010AA03A404, 2011AA03A101) and the Hong Kong Polytechnic University Grant (Grant No. J-BB9R).

REFERENCES

[1] Barry, T.L. (1968) Fluorescence of Eu^{2+}-activated phases in binary alkaline earth orthosilicate systems. *Journal of the Electrochemical Society*, **115**, 1181-1184. doi:10.1149/1.2410935

[2] Stefan, T., Peter, P., Gundula, R., Walter, T., Wolfgang, K. and Detlef, S. (2001) Light source comprising a light-emitting element. US Patent No. 6809347.

[3] Park, J.K., Lim, M.A., Kim, C.H., Park, J.T. and Choi, S.Y. (2003) White light-emitting diodes of GaN-based Sr_2SiO_4:Eu and the luminescent properties. *Applied Physics Letters*, **82**, 683-685. doi:10.1063/1.1544055

[4] Chen, L., Lin, C.C., Yeh, C.W. and Liu, R.S. (2010) Light converting inorganic phosphors for white light-emitting diodes. *Materials*, **3**, 2172-2195. doi:10.3390/ma3032172

[5] Kim, J.S., Park, Y.H., Choi, J.C. and Park, H.L. (2005) Optical and structural properties of Eu^{2+}-doped $(Sr_{1-x}Ba_x)_2SiO_4$ phosphors. *Journal of the Electrochemical Society*, **152**, H135-H137. dio:10.1149/1.1971065

[6] He, H., Fu, R.L., Zhang, X.L., Song, X.F., Zhao, X.R. and Pan, Z.W. (2009) Photoluminescence spectra tuning of Eu^{2+} activated orthosilicate phosphors used for white light emitting diodes. *Journal of Materials Science*: *Materials in Electronics*, **20**, 433-438. doi:10.1007/s10854-008-9747-5

[7] Lee, J.H. and Kim, Y.J. (2008) Photoluminescent properties of Sr_2SiO_4:Eu^{2+} phosphors prepared by solid-state reaction method. *Materials Science and Engineering B*, **146**, 99-102. doi:10.1016/j.mseb.2007.07.052

[8] Hsu, C., Jagannathan, R. and Lu, C. (2010) Luminescent enhancement with tunable emission in Sr_2SiO_4:Eu^{2+} phosphors for white LEDs. *Materials Science and Engineering: B*, **167**, 137-141. doi:10.1016/j.mseb.2010.01.045

[9] Zhang, X.G., Tang, X.P., Zhang, J.L. and Gong, M.L. (2010) An efficient and stable green phosphor $SrBaSiO_4$:Eu^{2+} for light-emitting diodes. *Journal of Luminescence*, **130**, 2288-2292. doi:10.1016/j.jlumin.2010.07.006

[10] Guo, H., Wang, X.F., Zhang, X.B., Tang, Y.F., Chen, L.X. and Ma, C.G. (2010) Effect of NH_4F flux on structural and luminescent properties of Sr_2SiO_4:Eu^{2+} phosphors prepared by solid-state reaction method. *Journal of the Electrochemical Society*, **157**, J310-J314. doi:10.1149/1.3454723

[11] Kang, H.S., Hong, S.K., Kang, Y.C., Jung, K.Y., Shul, Y.G. and Park, S.B. (2005) The enhancement of photoluminescence characteristics of Eu-doped barium strontium silicate phosphor particles by co-doping materials. *Journal of Alloys and Compounds*, **402**, 246-250. doi:10.1016/j.jallcom.2005.04.143

[12] Hsu, W., Sheng, M. and Tsai, M. (2009) Preparation of Eu-activated strontium orthosilicate ($Sr_{1.95}SiO_4$:$Eu_{0.05}$) phosphor by a sol-gel method and its luminescent properties. *Journal of Alloys and Compounds*, **467**, 491-495. doi:10.1016/j.jallcom.2007.12.014

[13] Lei, B.F., Machida, K., Horikawa, T. and Hanzawa, H. (2010) Facile combustion route for low-temperature preparation of Sr_2SiO_4:Eu^{2+} phosphor and its photoluminescence properties. *Japanese Journal of Applied Physics*, **49**, 095001-095006. doi:10.1143/JJAP.49.095001

[14] Chang, Y.L., Hsiang, H., Lan, F.T., Mei, L.T. and Yen, F.S. (2010) Synthesis of Sr_2SiO_4 nanometer particles from the core-shell precursor of $SrCO_3/SiO_2$. *Journal of Alloys and Compounds*, **500**, 108-112. doi:10.1016/j.jallcom.2010.04.002

[15] Hu, Y.S., Hao, J.H., Zhuang, W.D., Huang, X.W. and He, H.Q. (2011) Synthesis of (Sr,Eu)CO_3@SiO_2 core-shell-like precursor for alkali earth silicate phosphors. *Journal of Rare Earths*, **29**, 911-914. doi:10.1016/S1002-0721(10)60567-4

[16] Chrysafi, R., Perraki, T. and Kakali, G. (2007) Sol-gel preparation of $2CaO{\cdot}SiO_2$. *Journal of the European Ceramic Society*, **27**, 1707-1710. doi:10.1016/j.jeurceramsoc.2006.05.004

[17] Smith, J.V. and Bailey, S.W. (1963) Second review of Al-O and Si-O tetrahedral distances. *Acta Crystallographica*, **16**, 801-811. doi:10.1107/S0365110X63002061

[18] Ye, D.N., Li, Z. and He, W. (2001) Variation of the grand mean value of Si-O distances in metamorphic reactions. *Chinese Science Bulletin*, **46**, 702-704. doi:10.1007/BF03182841

[19] Park, J.H., Min, D.J. and Song, H.S. (2002) FT-IR Spectroscopic study on structure of $CaO-SiO_2$ and $CaO-SiO_2-CaF_2$ Slags. *ISIJ International*, **42**, 344-351. doi:10.2355/isijinternational.42.344

[20] Pieper, G., Eysel, W. and Hahn, T. (1972) Solid solubility and polymorphism in the system Sr_2SiO_4-Sr_2GeO_4-Ba_2GeO_4-Ba_2SiO_4. *Journal of American Ceramic Society*, **55**, 619-622. doi:10.1111/j.1151-2916.1972.tb13455.x

[21] Catti, M. and Gazzoni, G. (1983) The $\beta \rightleftarrows \alpha'$ phase transi-

tion of Sr_2SiO_4. II: X-ray and optical study, and ferroelasticity of the β form. *Acta crystallographica. Section B*, **39**, 679-684. doi:10.1107/S0108768183003225

[22] Sun, X.Y., Zhang, J.H., Zhang, X., Luo, Y.S. and Wang, X.J. (2008) A green-yellow emitting β-Sr_2SiO_4:Eu^{2+} phosphor for near ultraviolet chip white-light-emitting diode. *Journal of Rare Earths*, **26**, 421-424. doi:10.1016/S1002-0721(08)60109-X

[23] Nishioka, H., Watari, T., Eguchi, T. and Yada, M. (2011) Synthesis and luminescent properties of Sr_2SiO_4 phosphors. *IOP Conference Series*: *Materials Science and Engineering*, **18**, 102008. doi:10.1088/1757-899X/18/10/102008

[24] Lu, C.H. and Wu, P.C. (2008) Reaction mechanism and kinetic analysis of the formation of Sr_2SiO_4 via solid-state reaction. *Journal of Alloys and Compounds*, **466**, 457-462. doi:10.1016/j.jallcom.2007.11.066

[25] Wang, Z.J., Yang, Z.P., Guo, Q.L., Li, P.L. and Fu, G.S. (2009) Luminescence characteristics of Eu^{2+} activated Ca_2SiO_4, Sr_2SiO_4 and Ba_2SiO_4 phosphors for white LEDs. *Chinese Physics B*, **18**, 2068-2071. doi:10.1088/1674-1056/18/5/057

[26] Lee, S.H., Koo, H.Y. and Kang, Y.C. (2010) Characteristics of α'- and β-Sr_2SiO_4:Eu^{2+} phosphor powders prepared by spray pyrolysis. *Ceramics International*, **36**, 1233-1238. doi:10.1016/j.ceramint.2010.01.007

[27] Won, Y.S. and Park, S.S. (2010) Density functional theory study on two-peak emission of Eu^{2+} activators in Sr_2SiO_4. *Journal of Physics and Chemistry of Solids*, **71**, 1742-1745. doi:10.1016/j.jpcs.2010.09.008

[28] Nguyen, H., Yeo, I. and Mho, S. (2010) Identification of the two luminescence sites of Sr_2SiO_4:Eu^{2+} and $(Sr,Ba)_2SiO_4$:Eu^{2+} phosphors. *ECS Transactions*, **28**, 167-173. doi:10.1149/1.3367223.

